Effects of Heavy Element Abundance on Evolution of Supernova Remnants

Effects of Heavy Element Abundance on Evolution of Supernova Remnants

Masataka FUKUNAGA and Yutaka SABANO

Astronomical Institute, Faculty of Science,
Tohoku University, Sendai 980.

(Received April 15, 1980)

The evolution of supernova remnants is investigated numerically for the various abundances of the ambient medium in order to see the effects of a supernova explosion on the interstellar gas in various stages of the galactic evolution. It is shown that the time-evolution of a supernova remnant is delayed with the decrease in the heavy element abundance because of the suppressed cooling efficiency in the gas, and that the dynamical behavior of a remnant in the regime of z (the ratio of heavy element abundance to cosmic one) less than 10^{-2} is essentially the same as that in the case of no heavy element. The heavy element cooling also affects properties of dense shell behind the shock front, and the kinetic energy and the radius of a remnant. A discussion is given that the pressure in the hot gas, produced by supernova explosions, could be sufficiently high to support against the gravitational contraction in the initial phase of the Galaxy.

Keywords: Evolution of supernova remnant, Heavy element abundance.

§1. Introduction

It has been recognized that the supernova explosion plays an important role in the dynamics of the galactic gas, and also provides the heating and the ionizing sources of the galactic gas such as cosmic rays and X rays.[1] Hitherto many authors have studied the gas dynamics of supernova remnants[2,3,4] and the nature of the galactic gas which is dominated and regulated by supernova explosions has been discussed extensively.[5,6]

The previous investigations are, however, restricted to the "present" state of the galactic gas, which has the "Population-I abundance" of heavy elements. The heavy element abundance is considered to be increasing from nearly zero to the present cosmic abundance with supernova explosions in the course of the galactic evolution. Heavy elements affect the thermal and the dynamical behaviors of supernova remnents through its cooling ability. On the other hand the supernova remnants themselves consist of the galactic gas, affecting the properties of the galactic gas.

In the present paper we investigate numerically the evolution of supernova remnants for the various abundances of the ambient medium in order to see the effects of supernova explosions on the interstellar gas in various stages of the galactic evolution.

The model and some assumptions for numerical experiments are described in section 2, and the numerical results are presented in section 3. In section 4 the results are summarized and the implications of the results are discussed concerning the early evolution of the Galaxy.

§2. Model

We investigate the evolution of a supernova remnent using the following set of equations:

$$\frac{d\rho}{dt} = -\rho \nabla \cdot \boldsymbol{v} \tag{1}$$

$$\frac{d\boldsymbol{v}}{dt} = -\frac{1}{\rho}\nabla P, \tag{2}$$

$$\frac{dU}{dt} = -\rho L + \frac{P}{\rho^2}\frac{d\rho}{dt}, \tag{3}$$

$$\frac{dx}{dt} = -n_e x \alpha^{(2)}(T) + \zeta(1-x) + n_e(1-x)C(T), \tag{4}$$

and

$$P = n_t kT. \tag{5}$$

Here ρ, $\boldsymbol{v}$, P, and T are the mass density, the velocity, the pressure and the temperature of the gas, respectively. U is the internal energy per unit mass, L is the net cooling rate per unit mass, n_e is the electron number density, x is the ratio of the electron number density to that of hydrogen, n_t is the total number density of free particles, and k is the Boltzmann constant. The ratio of helium to hydrogen number density, n_{He}/n, is assumed to be 0.1, and the ionization degree of helium is adopted from the equilibrium calculation by Shapiro and Moore.[7] C(T) is the collisional ionization coefficient of hydrogen, $\alpha^{(2)}(T)$ is the hydrogen recombination coefficient excluding the recombination to the ground state, and ζ is the photoionization rate including both direct photoionization and ionizations by secondaries. The values of C(T) and $\alpha^{(2)}(T)$ are given by Spitzer,[1] and ζ is estimated from the cooling radiation as stated below.

We separate the cooling function into the light-element terms and the heavy-element term in order to see the effects of cooling by the heavy elements. Then the net cooling rate per unit mass consists of four terms:

$$L = L_H + L_{He} + L_z - L_{ph}, \tag{6}$$

where L_H, L_{He}, and L_z are the radiative loss by hydrogen atom, helium atom, and heavy elements, respectively. L_{ph} is the heating due to photoionization.

As for L_H we consider the loss due to collisional excitations, radiative recombination, and bremsstrahlung radiation, with the values given by Spitzer.[1] For L_{He} we take account of only the loss due to L_α-excitation (λ304Å), which is the important coolant at $T\sim10^5$K when the heavy element abundance is less than about 1/30 of the cosmic one, and we use the cooling rate given by Stern et al.[8] As for L_z we use the cooling rate given by Shapiro and Moore[7] for $T>2\times10^4$K, and by Dalgarno and McCray[9] for $T\leq2\times10^4$K both for cosmic abundance. In the temperature region, $10^4\lesssim T\lesssim10^{6.5}$K, the cooling by the collisional excitation of highly ionized heavy elements dominates the cooling by light elements for the cosmic abundance. In the region $T\lesssim10^4$K the cooling is only by the collisional excitation of low ionized heavy elements. In the region $T\gtrsim10^{6.5}$K, where bremsstrahlung is the main cooling process, the cooling by heavy elements is less by a factor of about 3 than that of light elements.

Obviously L_z is proportional to the amount of heavy elements, and we treat the ratio, z, of the total abundance of heavy elements to the cosmic one as a parameter to represent the amount of heavy elements. Here we assume simply a constant relative abundance among the elements, though it may change during the galactic evolution.

To estimate the photoionization rate, ζ, and the heating rate, L_{ph}, we have to calculate the photo-emissivity in the supernova remnant. Here we assume no ionizing photon comes from outside the remnant. We compute the ionization rate for two energy ranges, 13-41 eV and 41-150 eV. Beyond 150 eV, the luminosity and absorption cross-section are small. The mean energy in the former range is about 26 eV, which is sufficiently low that ionization by secondaries can be neglected. The mean energy for the latter range is taken to be 100 eV, and the data on the heating energy and the number of secondary ionizations produced per photoionization are given in Dalgarno and McCray.[9] The radiation spectrum as a function of temperature is estimated from the work by Stern et al.[8] using equilibrium calculations of ionization degrees by Jordan.[10]

We neglect the radiative transfer, which is important when a dense cool shell has formed, and assume the whole remnant is optically thin to the ionizing radiation, if not mentioned especially. We also consider another case that the dense shell is completely thick ($\zeta=0$) after the formation of the neutral shell. As will be discussed in section 3-b, the dynamics of supernova remnants is scarcely different between the tow cases.

For numerical computations we assume spherical symmetry and the time evolution of a supernova remnant is pursued by a one-dimensional Lagrangian hydrodynamic program with artificial viscosity. Initially the supernova energy E_0 is deposited as a heat in a uniform medium with density n_0 and temperature T_0 in a similar way to Chevalier.[3] Computer runs were performed for $E_0=3.7\times10^{50}$erg, and the temperature of the ambient medium was assumed to be 10^4K and pre-ionized, while the initial density and heavy element abundance

in the medium were assumed to have various values likely to occur in the galactic evolution. The results for other choise of E_0 can be obtained by scaling the computed results.[3,4] Lagrangian mesh points were used between 80-120, and rezoning of the mesh points was carried out during the expansion of the blast wave.

§3. Results

a) Evolution of supernova remnant in a medium with cosmic abundance

As the evolution of a supernova remnant in the case of z=1 has been discussed in detail by previous authors, we here briefly inspect this case for comparison with other cases. The results of numerical calculation for $n_0=0.1$ cm^{-3} are displayed in Fig. 1-a, b, and c, where the hydrogen number density n, the temperature T, and the pressure of the gas are plotted against the radial distance R, respectively at four epochs. Until the first epoch, (1) 9.71×10^4 years after the supernova explosion, radiative cooling is not yet important and the situation is well described by the adiabatic similarity solution given by Sedov.[12] When the temperature of the shock front decreases down to about 5×10^5K, the cooling by heavy elements causes the temperature to drop behind the shock front at epoch (1). Because of the drop in pressure, a cool dense shell forms behind the shock front at epoch (2), 15.28×10^4years, when the density of the shell reaches its maximum. After this epoch the velocity of the shock front decreases, hence the pressure in the dense shell falls, giving less compression. The density in the shell decreases gradually, while the mass of the shell increases (see the results at (3) and (4) in Fig. 1-a. The temperature of the dense shell decreases slowly to about 5000 K at the epoch (4), about 10^6years after the explosion.

Fig. 2 shows the radius R_s of the shock front, as a function of time, and Fig. 3 shows the temperature T_s of the shock front as a function of the radius (see the curves for z=1). In the adiabatic phase R_s is well approximated by the Sedov solution, $R_s\propto t^{2/5}$, which is represented by the left thin straight line in Fig. 2, and by the thin straight line in Fig. 3, respectively. When the shock front temperature drops to about 5×10^5K, the pressure behind the shock front drops because of rapid cooling as stated above. The gas flows into the pressure dip, so the velocity of the shock front decreases, departing from the Sedov solution. The shock temperature drops rapidly until the density of the shell reaches its maximum. This transient phase corresponds to a isothermal spherical shock solution,[13] $R_s\propto t^{1/4}$. The shell loosen after the maximum density, and then the velocity of the shock front, hence the shock temperature also increases slightly, as seen in Fig. 3. In the last phase the shock front propagates approximately as $R_s\propto t^{1/3}$, which is represented by the right thin line in Fig. 2. This relation coincides with that given by Chevalier,[3] $R_s\propto t^{0.32}$, at the same phase for the case $n_0=0.01$ cm^{-3} and z=1, or $R_s\propto t^{0.31}$ for $n_0=1$ cm^{-3} and z=1 case. This last phase will continue until the velocity of the shock

front approaches the sound velocity of the ambient medium.

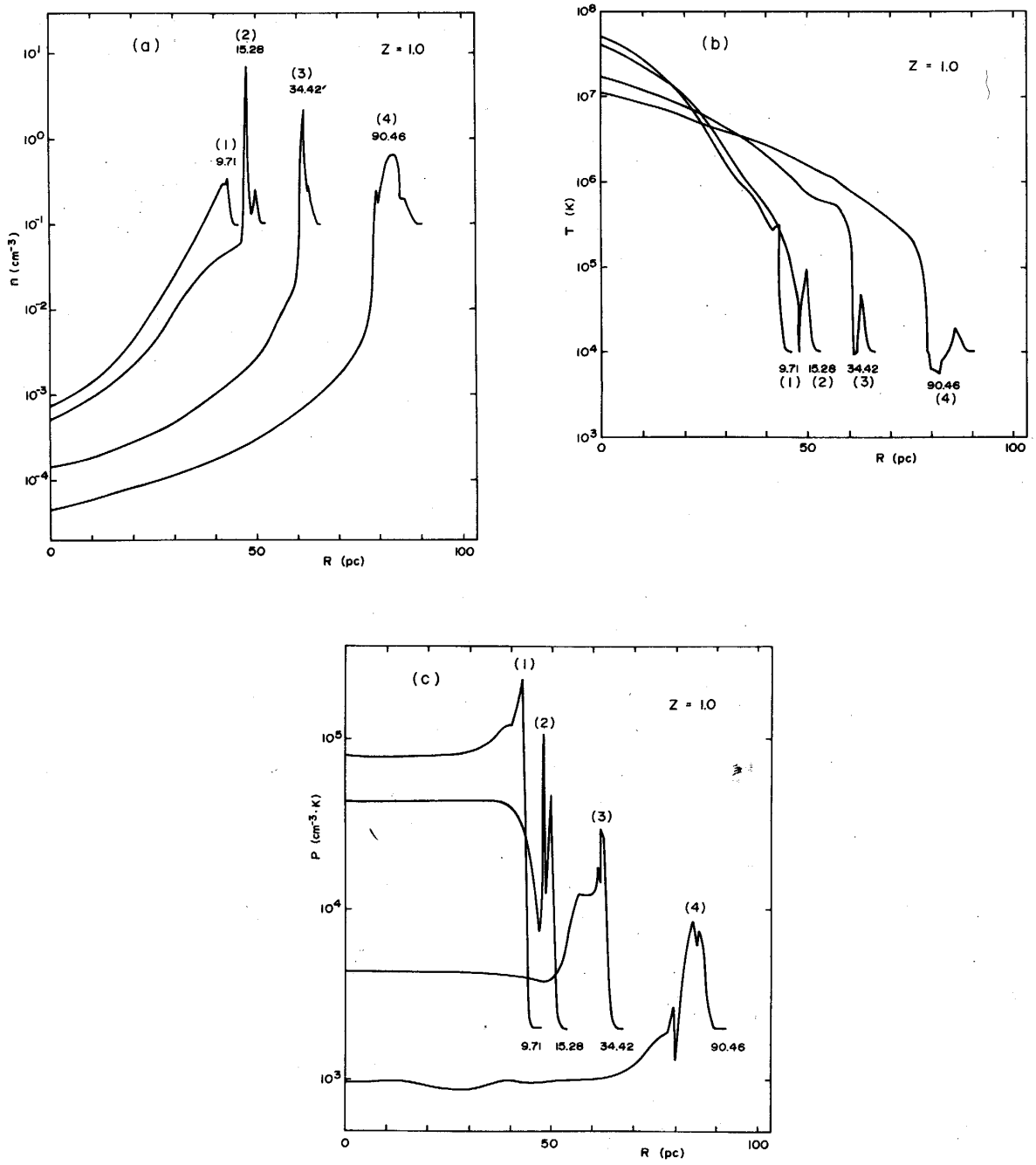

Fig. 1-a, b, and c. Profiles of (a) hydrogen number density, n; (b) temperature, T; and (c) gas pressure, P, at four epochs in the evolution of a 3.7×10^{50} erg supernova explosion in a medium with z=1, $n_0=0.1$ cm^{-3} and $T_0=10^4$K. Each curve is labelled by the time elapsed after the supernova explosion in units of 10^4yr.

b) Effects of heavy element abundance

Computer runs were performed for various values of z in the possible range, $0 \leq z \leq 1$. If z is less than about 1/30, the He cooling dominates the cooling by heavy elements at $T \sim 10^5$K, and the cooling efficiency does not depend on z. Therefore the evolutions in the case of z less than about 10^{-2} can be almost the same as that in the case of z=0. This is confirmed by numerical results. We here inspect the characteristic three cases of z=0, 0.1, and 1 all for $n_0=0.1$ cm^{-3} as the representatives.

Figs. 2 and 3 display the results for z=0, and 0.1 as well as those for z=1 which is discussed in the previous subsection. As shown in the figures, the decrease in z results in the delay of the evolutionary phases such as the shell formation epoch, though the qualitative features of the evolution are not changed.

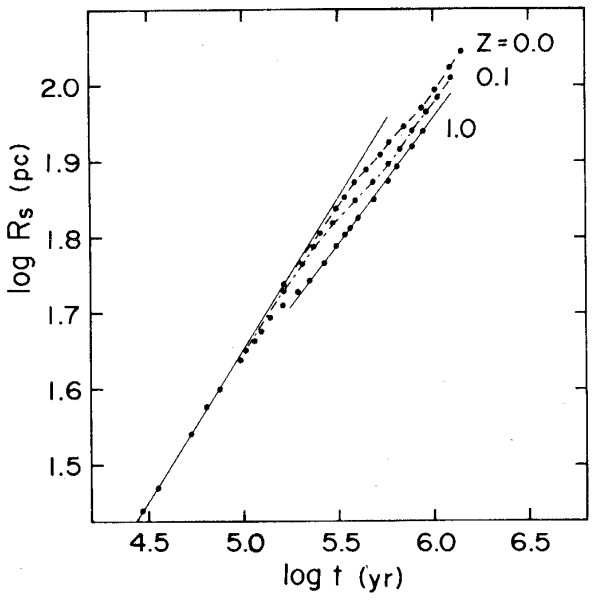

Fig. 2. The radius of the shock front as a function of time for the three cases of z. The left thin straight line represents the Sedov solution, $R_s \propto t^{0.4}$, and the right one represents the relation, $R_s \propto t^{1/3}$.

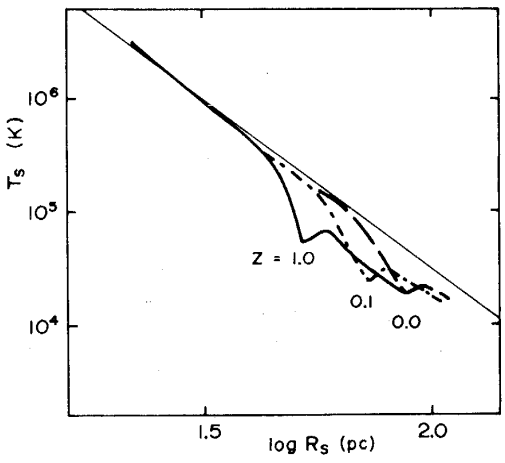

Fig. 3. The temperature T_s of the shock front as a function of the radius for the three cases of z. The thin straight line represents the Sedov solution.

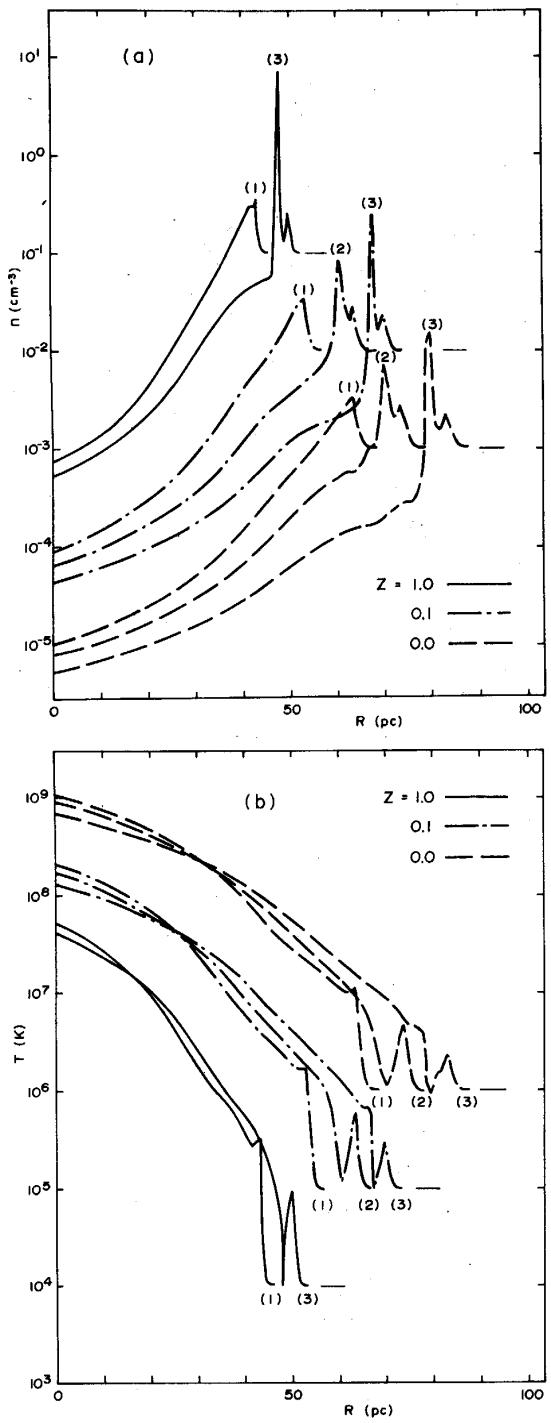

Fig. 4-a and b. Profiles of (a) hydrogen number density n, and (b) temperature at the three characteristic epochs for the three cases of z. The given values of the ordinate are for the case of z=1. The curves for z=0.1 and 0 are shifted downward in Fig. 4-a, and upward in Fig. 4-b, by one and two orders of magnitude, respectively. The thin level lines represent the ambient interstellar values, n_0=0.1 cm^{-3} and T_0=10^4K. The time of each epoch is given in Table 1. Epoch (2) for z=1 is omitted for greater clarity.

Table 1. Characteristic times and the radius for the three cases of z

z	t_1(yr)	R_1(pc)	t_2(yr)	R_2(pc)	t_3(yr)	R_3(pc)	(t_3-t_1)(yr)	n_{max}/n_0
1.0	0.97×10^5	43.6	1.39×10^5	49.4	1.53×10^5	50.3	0.56×10^5	70
0.1	1.64	53.7	2.97	66.0	3.87	70.8	2.23	25
0.0	2.56	63.6	3.89	74.7	5.86	84.4	3.30	15

Fig. 4-a shows the density profiles at some epochs for the three values of z. The given values of the ordinate are hydrogen number density for the case z=1. The curves for z=0.1 and 0 are shifted downward by one and two orders of magnitude in the ordinate scale, respectively. Each profile represents the characteristic epoch: (1) is the epoch when the temperature behind the shock front first drops lower than that of the shock front, $t=t_1$, (2) is when the dense shell forms with the temperature decreased to about 10^4K, $t=t_2$, (for z=1 the density profile at this epoch is not represented because it is very close to that at $t=t_1$), and (3) is when the density of the shell reaches its maximum, $t=t_3$. The times elapsed after the supernova explosion till each epoch as well as the shell formation time, t_3-t_1, are given in Table 1. The table also lists the radii of shock fronts at each epoch for the three cases. The delays of the characteristic epochs and the longer shell formation time for the smaller value of z is obviously attributed to longer cooling time for smaller z, and hence the radii at the characteristic epochs become larger for smaller z.

The last column of Table 1 is the ratio n_{max}/n_0, of the maximum density of the shell to the ambient density. If we assume an isothermal shock at the shell formation epoch, the ratio is given by $n_s/n_0=v_s^2/c_0^2$, where v_s is the velocity of the shock front and c_0 is the sound speed in the ambient gas, hence the difference in the maximum density of the shell can be explained by that of the shock speed when the effective cooling acts in the shell.

Fig. 4-b shows the temperature profiles at the same epochs as in Fig. 4-a for the three cases of z. The temperature values of the ordinate are for z=1.0. The curves for z=0.1 and 0.0 are shifted upward by one and two orders of magnitude, respectively. It is remarkable that the temperature in the dense shell behind the shock front at the epoch (3) is about 10^4K for all cases of z contrary to the case $n_0=1$ cm^{-3} and z=1 for which the numerical calculation shows that the shell temperature rapidly drops to $10\text{-}10^2$K at the shell formation epoch.[3,4] The temperature of the shell is practically determined by the balance condition between the radiative cooling by heavy elements such as C^+, O, Fe^+, and Si^+, and the heating by photoionization. Since the dense shell becomes optically thick to the hard-ultraviolet radiation, our assumption of optically thin is invalid then, and this may cause the shell temperature high unreasonably. The assumption is, however, appropriate as following. We can

estimate the behavior of the optically thick shell setting $\zeta=0$, then the temperature of the shell drops within the cooling time scale $3\times10^6(n_s z)^{-1}$years provided that $x=10^{-2}$. For $n_s z\sim3$, the typical value for the $n_0=0.1$ cm^{-3} and $z=1$ case, the cooling time scale is about 10^6 years, which is approximately the same as the dynamical time scale of the supernova remnant. The cases of further small $n_0 z$ ($n_0 z<<1$ cm^{-3}) the cooling time in the shell, of cause, exceeds the evolution time, hence the formed shell will be relatively warm ($T\sim10^{3\text{-}4}$K) and rarefied ($n_s/n_0\sim10$) regardeless of the optical thickness, as confirmed by several numerical calculations for various values of $n_0 z$ less than 0.1. Thus it seems that dense, cold shell as the interstellar "standard cloud"[1] does not forms during the evolution of supernova remnants in the interstellar medium of low $n_0 z$.

The abundance of heavy elements also affects the energetics of a whole supernova remnant. The energetics for the three cases of z are represented as a function of the remnant radius in Fig. 5, where the curves labeled by E_{kin} represents the kinetic energy, the curves in the middle represent E_{kin} plus the internal energy E_{int}, and the curve labeled by E_{tot} represents the total energy within a supernova remnant all in units of the initial supernova energy E_0. (E_{tot} minus the curve $E_{kin}+E_{int}$ denotes the energy radiated away). The total energy increases due to the internal energy added by surrounding gas which is assumed to be ionized and $T=10^4$K. The kinetic energy is conserved in the adiabatic phase, increases temporarily when the material is accelerated into the dense shell, then decrease because of dissipation at the shock front. The internal energy is radiated away in the cooling phase, vastly in a shell formation epoch, then turn to increase because of expansion into the surrounding gas and the decrease of cooling efficiency by radiation. The small temporal increase of E_{kin} and rapid decrease of E_{int} are more prominent for large z.

In the case of small z a large amount of the internal energy remains in the inner hot region, and the kinetic energy is transported to the larger radius. The results show that the decrease in the kinetic energy after the epoch of the maximum shell density is approximated by $E_{kin}\propto R_s^{-2.6}$ independently of z values. If we estimate the kinetic energy available to stir up the interstellar medium as that at the time when the shell velocity has slowed down to 14 km s^{-1}, the rms velocity of random motion of the interstellar cloud,[1] it is found to be 6, 8, and 10 percent of the initial supernova energy for $n_0=1$ cm^{-3} and for $z=1$, 0.1, and 0.0, respectively. If the ultimate radius of a supernova remnant is limited to a certain range, say $R_s\sim100$ pc, because of, for example, coarescence with other remnants, the available kinetic energy is 6, 10, and 17 percent for $z=1$, 0.1, and 0.0, respectively. Any how the supernova remnants supply the larger kinetic energy accordingly as the heavy element abundance decreases.

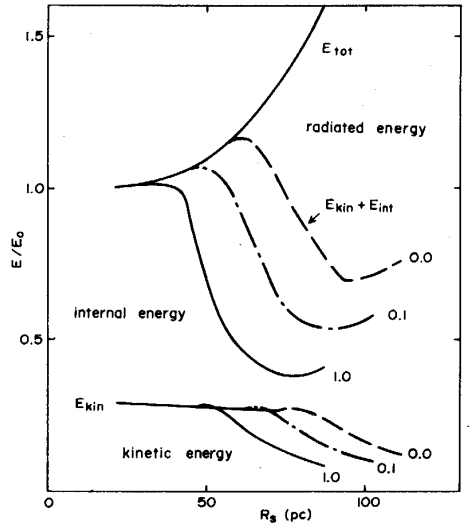

Fig. 5. The energetics for the three cases of z as a function of the remnant radius R_s. The curves labeled by E_{kin} represent the bulk kinetic energy, the curves in the middle represent E_{kin} plus the internal energy E_{int}, and the curve labeled by E_{tot} represents the total energy within a supernova remnant all in units of the initial supernova energy E_0.

§4. Summary and Discussion

In the present paper the evolution of a supernova remnant is pursued numerically for the various abundances of the ambient medium. The results are summarized as follows:

(1) If the abundance of the heavy elements is low, the cooling rate at $T\sim10^{4.0-6.5}$K is reduced so that the dynamical evolution of a supernova remnant is delayed. The cooling by the heavy elements at high temperature of $T>10^4$K is negligible compared with the cooling by H and He atom if $z<<3\times10^{-2}$, then the evolutionary features are similar to the metal free case of z=0.

(2) Since the cooling at low temperature of $T<10^4$K is also reduced in the medium of the low heavy element abundance, the physical properties of the shell formed behind the shock front markedly differ from the case of z=1 and $n_0=1$ cm^{-3}. The temperature T_s and the density n_s in the shell have the values of $T_s\sim10^4$K and $n_s/n_0\sim10$, respectively, in the case of $n_0z<<1$, while $T_s\sim10^2$K and $n_s/n_0\sim10^4$ in the case of $n_0z=1$.

(3) The kinetic energy of the remnant is estimated at the time when the shell velocity has slowed down to 14 km s^{-1}, the rms velocity of the random motion in the interstellar gas. It becomes larger as the heavy element abundance decreases.

(4) The final radius, R_{SNR}, of a remnant when the shell velocity reaches 14 km s^{-1} also becomes larger for the lower values of z. The final radius of z=0 is found to be 25 percent larger than that of z=1.

To consider the effects of supernova explosions on the galactic evolution, we now introduce a parameter f defined as $f=V_{SNR}B_{SN}\tau_{SNR}/V_G$, where V_{SNR} is the volume of a supernova remnant, τ_{SNR} is the life time of a supernova remnant, B_{SN} is the birth rate of supernovae in the Galaxy, and V_G is the volume of the Galaxy. The parameter f means the filling factor of supernova remnants in the Galaxy if f<1.

The value of f under the "present" condition of the Galaxy is estimated as $f\sim 0.06$. Here R_{SNR} is given by the present computation for z=1 on $n_0=1$ cm^{-3}, the mean gas density in the galactic disk, then V_{SNR} is $2\times10^5 pc^3$. τ_{SNR} is the cooling time scale of the hot interior of a remnant. V_G is 1.3×10^{11} pc^3 if the Galaxy has a radius of 15 kpc and the thickness of 200 pc. B_{SN} is $\sim 1/30$ y^{-1} in the "present" Galaxy.[1] The above value of f shows that the hot gas in the supernova is isolated in the galactic disk.

In the early phase of the galactic evolution, both the gas density and the heavy element abundance are supposed to have lower values, and the birth rate of supernovae is higher than that at the "present" Galaxy. These all make the value of f larger, and the state of the galactic gas will be much different from the "present" interstellar gas. We here consider the initial contracting phase of the Galaxy adopting the evolutionary model of Daido,[14] which can properly explain the distribution of the heavy element abundance in the halo objects. In the early phase of the galactic contraction, the galactic radius, the hydrogen number density, and the heavy element abundance are $\sim$50 kpc, $\sim 10^{-2} cm^{-3}$, and less than 10^{-2}, respectively. The time scale, $V_G/V_{SNR}\ B_{SN}$, in which the filling factor becomes 1 is 1×10^8 years, which is somewhat shorter than the free-fall time, 3×10^8 years, of the overall Galaxy with the mass $2\times10^{11} M_\odot$ and the initial radius 50 kpc. Therefore the filling factor of the hot gas will eventually exceeds 1 before the contraction completes. The newly formed supernovae are to explode in the hot gas. The galactic gas is heated further and kept at high temperature of 10^6K, and the cooling time scale is $\gtrsim 10^9$ years, much larger than the free-fall time. The pressure of the hot gas will sufficiently high to support against the gravitational contraction, and the initial contraction of the Galaxy is supposed to be much slower than the free-fall contraction due to gravitation. This conclusion is compatible with the "slow' contraction model obtained from the kinematical study of old stars[15] and from the study of the chemical evolution of the Galaxy.[14]

The authors would like to express their gratitude to Professor K. Takakubo for a critical reading of the manuscript. The authors also thank Miss M. Nakamura for typing the manuscript and preparing the drawings. The numerical computation were carried out on the ACOS 77 NEAC 700 at the Computer Center of Tohoku University.

References

1) L. Spitzer, Jr.: Physical Processes in the Interstellar Medium (A Wiley-Interscience Publication, New York 1978).
2) D.P. Cox: Astrophys. J. 178 (1972) 159.
3) R.A. Chevalier: Astrophys. J. 188 (1974) 501.
4) V.N. Mansfield and E.E. Salpeter: Astrophys. J. 190 (1974) 305.
5) C.F. McKee and J.P. Ostriker: Astrophys. J. 218 (1977) 148.
6) B.W. Smith: Astrophys. J. 211 (1977) 404.
7) P.R. Shapiro and R.T. Moore: Astrophys. J. 207 (1976) 460.
8) R. Stern, E. Wang and S. Bower: Astrophys. J. Suppl. 37 (1978) 195.
9) A. Dalgarno and R. McCray: Ann. Rev. Astron. Astrophys. 10 (1972) 375.
10) C. Jordan: Monthly Notices Roy. Astron. Soc. 142 (1969) 501.
11) D. Richtmyer and K.W. Morton: Difference Methods in Initial-Value Problems (Interscience Publishers, New York 1967).
12) L.T. Sedov: Similarity and Differential Methods in Mechanics (Academic Press, New York 1959).
13) J.H. Oort: Problems of Cosmical Aerodynamics (Central Air Document Office, Dayton, Ohio 1951).
14) T. Daido: Publ. Astron. Soc. Japan 32 (1980) 63.
15) Y. Yoshii and H. Saio: Publ. Astron. Soc. Japan 31 (1979) 339.